RSC Advances

PAPER

View Article Online
View Journal | View Issue

Cite this: *RSC Adv.*, 2015, **5**, 8345

Two-step spray-drying synthesis of dense and highly luminescent YAG:Ce^{3+} phosphor powders with spherical shape†

Jung Sang Cho,‡[a] Kyeong Youl Jung‡[b] and Yun Chan Kang*[a]

Received 11th November 2014
Accepted 15th December 2014

DOI: 10.1039/c4ra14302g

www.rsc.org/advances

Two-step spray drying using a commercially available spray dryer was carried out to prepare dense and spherical $Y_3Al_5O_{12}$:Ce^{3+} (YAG:Ce^{3+}) particles with good luminescence characteristics. Hollow YAG:Ce^{3+} powder particles with a thin shell were first obtained by the spray drying of an aqueous precursor solution containing citric acid as an organic additive. The powder was then pulverized into nanoparticles measuring tens of nanometers in size by ball milling. The second spray drying using a colloidal solution of the nanometer-sized precursor powder made it possible to successfully produce spherical YAG:Ce^{3+} particles with an average size of 2–3 μm. After thermal treatment at a high temperature between 1200 and 1400 °C, spherical YAG:Ce^{3+} particles with a pure phase and dense structure were obtained. These particles were shown to have good luminescence characteristics suitable for the fabrication of white light-emitting diodes.

Introduction

White light-emitting diodes (W-LEDs) have attracted attention for potential application in indoor/outdoor lighting, lamps for vehicles, backlights for display devices, *etc.*, because they have high efficiency, very long lighting lifetime, and low power consumption.[1–5] Currently, commercially available W-LEDs are generally fabricated by coating a yellow phosphor powder onto blue-emitting InGaN LED chips because yellow phosphors convert a portion of blue light into yellow light before white light is generated.[6,7]

Among the phosphor powders developed in the past decades, Ce^{3+}-doped yttrium aluminum garnet ($Y_3Al_5O_{12}$:Ce, YAG:Ce^{3+}) has been widely utilized as the yellow-emitting phosphor for W-LEDs because of its excellent luminescence property.[4,8–10] To develop more efficient W-LEDs, it is important to prepare YAG:Ce^{3+} phosphor powder with high photoluminescence intensity. The luminescence properties of phosphors strongly depend on the physical properties, such as specific surface area, crystallinity, particle size, size distribution, and morphology, of their host materials. In particular, the required particle size of YAG:Ce^{3+} yellow phosphor continues to decrease in order to maintain the high luminescence properties required to improve the efficiency, reproducibility of color purity, and production yield of W-LEDs. As a result, several approaches, including the sol–gel, hydrothermal, co-precipitation, solvothermal, and molten salt methods, have been used to synthesize YAG:Ce^{3+} phosphor powders. Most of these synthesis routes can be classified into two groups according to the processing method: solid-state and wet-state reactions.[10–16] In general, commercial YAG:Ce^{3+} phosphor powder is synthesized by a solid-state reaction using precursor powders of Y_2O_3, Al_2O_3, and CeO_2 at high temperatures above 1600 °C for an extended period.[10,17,18] However, the resulting product has certain disadvantages such as inhomogeneous phase distribution, large particle size, and non-uniform particle shape. Meanwhile, fine YAG:Ce^{3+} phosphor powders could be synthesized *via* wet-state reactions using water-soluble inorganic precursors.[11,19–21] However, the resulting powders exhibit agglomerated structures, which are unavoidable because a post-reaction thermal sintering at a high temperature above 1200 °C is required to obtain high luminescence properties. Therefore, it is necessary to develop a new strategy that is cost effective and makes it possible to produce agglomeration-free, spherical, and dense YAG:Ce^{3+} powder with fine particles and high luminescence.

Spray-drying processes have been widely used in the ceramics industry to produce a dried powder from a liquid solution or suspension.[22–28] The process is simple and cost effective, and it can be easily scaled up to produce powder in volumes that can be measured in tons. However, typical spray-dried powders have hollow structures because the fast drying step leads to a solute-concentration gradient, which is bound to

[a]*Department of Materials Science and Engineering, Korea University, Anam-Dong, Seongbuk-Gu, Seoul 136-713, Republic of Korea. E-mail: yckang@korea.ac.kr; Fax: +82-2-928-3584*

[b]*Department of Chemical Engineering, Kongju National University, 275 Budae-Dong, Cheonan, Chungnam 330-717, Republic of Korea*

† Electronic supplementary information (ESI) available. See DOI: 10.1039/c4ra14302g

‡ These authors contributed equally to this work.

induce surface precipitation. When spray drying is used directly to prepare YAG:Ce^{3+} powder, hollow structures are inevitably produced, which makes it harder to obtain high photoluminescence properties. Therefore, it remains a significant challenge to develop a new spray-drying process that produces fine, non-aggregating, and solid-core YAG:Ce^{3+} phosphor powder with high photoluminescence.

In this study, a two-step spray-drying process was applied for the large-scale production of dense and spherical YAG:Ce^{3+} phosphor microspheres. By using the spray-drying process, phase-pure YAG:Ce^{3+} particles could be formed at a relatively lower sintering temperature than that required for a conventional solid-state reaction method owing to the homogeneous mixing of each component of YAG:Ce^{3+} on the nanometer scale. An aqueous spray solution containing an organic additive was first prepared, with each component of the phosphor mixed homogeneously at the molecular level. In the first step, a precursor powder of the multicomponent YAG:Ce^{3+} phosphor was prepared as hollow particles with a very thin shell structure by spray-drying the prepared solution. After the mixed precursor powder was calcinated at a low temperature, it was wet-milled to pulverize the hollow YAG:Ce^{3+} into particles measuring tens of nanometers in size. A highly stable colloidal solution was then prepared from these nanometer-sized particles. Thereafter, the second spray drying of the suspension was carried out, followed by sintering at high temperature to produce phosphor microspheres with dense structures and good photoluminescence. Changes in the physical, morphological, and photoluminescence properties of the YAG:Ce^{3+} phosphor microspheres during the two-step spray-drying process were investigated systematically.

Experimental

Sample preparation

A commercial spray-drying system (Fig. S1†) was used to prepare the YAG:Ce^{3+} precursor powder particles with a thin-walled hollow structure. A spray solution consisting of the yttrium, aluminum, and cerium components was pumped into an atomizing device, where it was transformed into a spray of small droplets. This spray solution was prepared by dissolving yttrium oxide (Y_2O_3, 99.9%, Rhodia), aluminum nitrate nonahydrate [$Al(NO_3)_3 \cdot 9H_2O$, 98%, Aldrich], and cerium nitrate hexahydrate [$Ce(NO_3)_3 \cdot 6H_2O$, 99%, Aldrich] in distilled water. The concentration of Ce activator was fixed at 6.4 mol% of Y^{3+}. Citric acid (CA, $C_6H_{10}O_8$, Junsei) was also added to the above solution to form the thin-walled hollow precursor powder particles. The total concentration of metal components in the spray solution was fixed at 0.5 M, and the concentration of citric acid was also fixed at 0.5 M. The transformed small droplets were then brought into contact with a stream of hot air, which resulted in rapid evaporation of the moisture while the droplets were still suspended in the drying air. The dried powder was separated from the humid air by centrifugal forces in a cyclone system. The centrifugal separation was initiated by the marked increase in air speed when the mixture of particles and air entered the cyclone system. The temperatures at the inlet and outlet of the spray dryer were 250 and 120 °C, respectively. A two-fluid nozzle was used as an atomizer, and the atomization pressure was 0.8 bar.

The obtained precursor powder was calcined at 550 °C for 3 h in air and then ball-milled for 5 h in deionized water to prepare a suspension for the second round of spray drying. The prepared suspension was spray-dried again at 250 °C to produce microspheres. In the spray-drying setup, the feeding suspension was pumped into the atomizing device and then dispersed as aerosol droplets. With the hot air flowing, the moisture evaporated in a very short time and spherical powder particles were produced. The obtained powder was then sintered in a tube furnace at various temperatures between 1200 and 1400 °C for 3 h under the reducing atmosphere of 5% H_2/Ar with the flow rate of 500 ml min^{-1}.

Characterizations

The microstructures of the produced powders were observed by scanning electron microscopy (SEM; JSM-6060, JEOL), field-emission transmission electron microscopy (FETEM; JEM-2100F, JEOL), and high-resolution transmission electron microscopy (TEM; JEOL-2100F, JEOL). The crystal phases of the powders were evaluated by an X-ray diffractometer (XRD; X'Pert PRO MPD, PANalytical) using Cu K_α radiation (l = 1.5418 Å) at the Korea Basic Science Institute (Daegu). The surface areas of the powders were measured by the Brunauer–Emmett–Teller (BET) method using N_2 as the adsorbate gas. Thermogravimetric (TG) analysis was performed using a thermogravimetric analyzer (Pyris 1 TGA, PerkinElmer) in the temperature range of 25–650 °C at a heating rate of 10 °C min^{-1} under a static air atmosphere. The photoluminescence spectra were measured by a spectrophotometer (LS 50, PerkinElmer) using a Xe flash lamp as an excitation light source. An image analyzer (ImageJ, NIH) was used to determine the particle-size distributions of the powders.

Results and discussion

Fig. 1 shows SEM and TEM images of the as-prepared YAG:Ce^{3+} precursor powder after the first spray drying. As one can see from the SEM data (Fig. 1(a)), the precursor powder consisted of hollow spheres with a thin shell. This hollow-structured morphology developed because the surface precipitation began first and insufficient gas diffusion through the shell layer inflated the droplets during the drying step. Some of particles displayed fractured structures because the thin layer formed by the surface precipitation burst as the internal pressure became elevated. As a result, the obtained powder showed bimodal size distribution in which most of the powder particles were larger than 10 μm. The precursor powder prepared by the first spray drying was an organic–inorganic composite containing yttrium, aluminum, and cerium salts, with CA used as a chelating agent. Calcination was necessary to eliminate the CA and thermally decompose nitrate salts precipitated in the precursor powder. To determine the optimal calcination

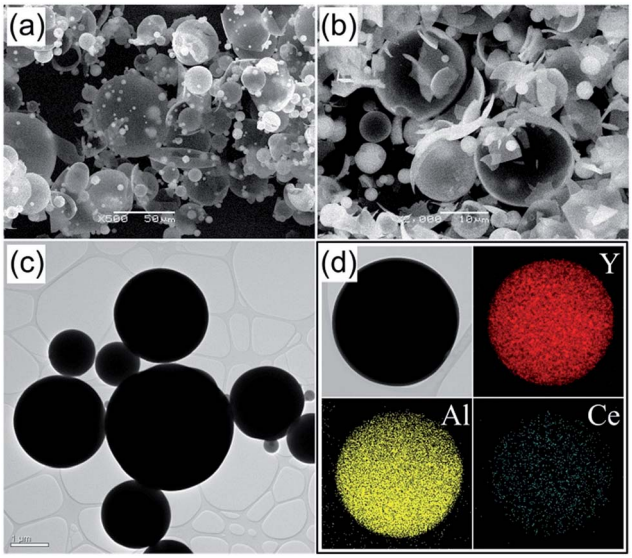

Fig. 1 Morphologies and elemental mapping images of the YAG:Ce^{3+} precursor powders before and after calcination at 550 °C: (a) SEM image of spray-dried precursor powders, (b) SEM image of calcined powders, (c) TEM image of calcined powders, and (d) elemental mapping images of calcined powders.

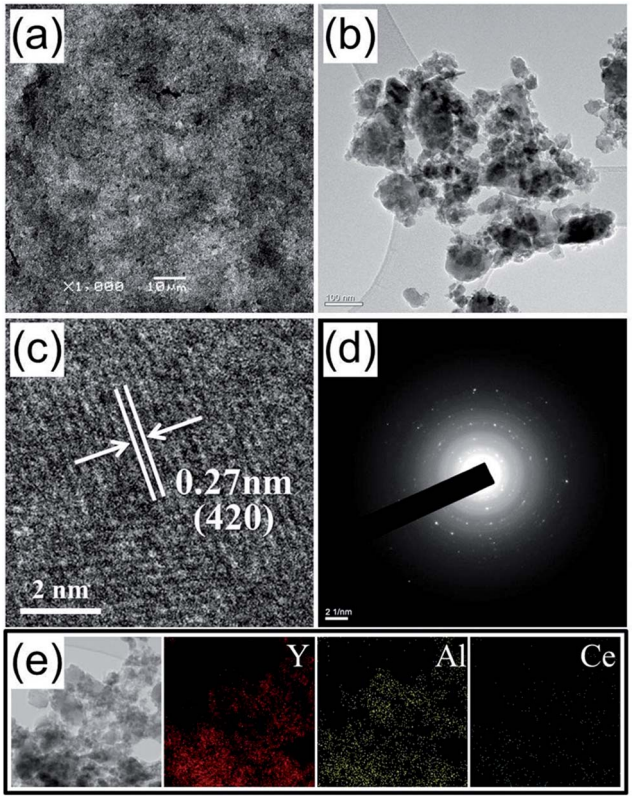

Fig. 2 Morphologies and elemental mapping images of the crushed YAG:Ce^{3+} powders after planetary-milling process: (a) SEM image, (b) TEM image, (c) HR-TEM images, (d) SAED pattern, and (e) elemental mapping images.

temperature, the thermal decomposition behavior of the precursor particles was investigated by TG analysis. Fig. S2† shows the weight loss of the prepared YAG:Ce^{3+} precursor powder with increasing temperature. Owing to the evaporation of adsorbed water molecules, 12 wt% was lost up to a temperature of about 100 °C. In the temperature range from 100 to 320 °C, a weight loss of 30 wt% was recorded as a result of the burning of the CA additive and decomposition of the nitrate salts in the precursor powder. Finally, a weight loss of 22 wt% occurred between 320 and 550 °C owing to the decomposition of carbon residues in the spray-dried precursor powder. Based on this result, we determined that 550 °C was the optimal calcination temperature to completely eliminate the decomposable materials from the precursor powder. In Fig. 1(b), the powder particles after calcination at 550 °C exhibited a hollow structure with a thin wall, which is similar to the structure before calcination. However, some powder particles were fractured during the calcination because the wall was weak and easily fragmented by the thermal shock. In addition, small particles with filled structures, as confirmed by the TEM image in Fig. 1(c), were also observed. As shown in the dot mapping images in Fig. 1(d), the yttrium, aluminum, and cerium components of the YAG:Ce^{3+} phosphor powder were distributed homogeneously in the structure.

The YAG:Ce^{3+} precursor powder obtained after calcination was crushed by zirconia balls in a planetary milling process to prepare nanoparticles for the second spray-drying step. It was easy for the calcined powder to be pulverized to nanometer-sized particles by simple ball milling. The resulting powder particles measured several tens of nanometers in size, as shown by the SEM and TEM images in Fig. 2(a) and (b). In the high-resolution TEM image (Fig. 2(c)), however, clear lattice planes of the crystal structure were not observed. Moreover, the selected-area electron diffraction (SAED) result (Fig. 2(d)) indicates that the ball-milled precursor YAG:Ce^{3+} nanoparticles were either in the amorphous phase or had low crystallinity because they were calcined at 550 °C. Fig. 2(e) shows elemental-mapping images of Y, Al, and Ce in the crushed nanoparticles, indicating that all constituting elements of the YAG:Ce^{3+} phosphor were distributed uniformly throughout the nanoparticles without any phase separation.

In order to produce spherical granules with dimensions of several micrometers, a second round of spray drying was conducted using a stable colloidal suspension that was prepared with the YAG:Ce^{3+} nanoparticles obtained by wet ball-milling. Fig. 3(a) shows SEM images of the prepared granules after the second spray drying. The granules consisting of nanometer-sized primary particles had an agglomeration-free spherical shape and an average size of about 3.3 ± 0.9 μm. These granular particles did not show luminescence because of their low crystallinity and there was no activation of Ce^{3+} ions. According to the literature on YAG:Ce^{3+} phosphor, heat treatment at a temperature above 1200 °C is necessary for YAG:Ce^{3+} phosphor to acquire high photoluminescence.[29,30] Therefore, the granule powders

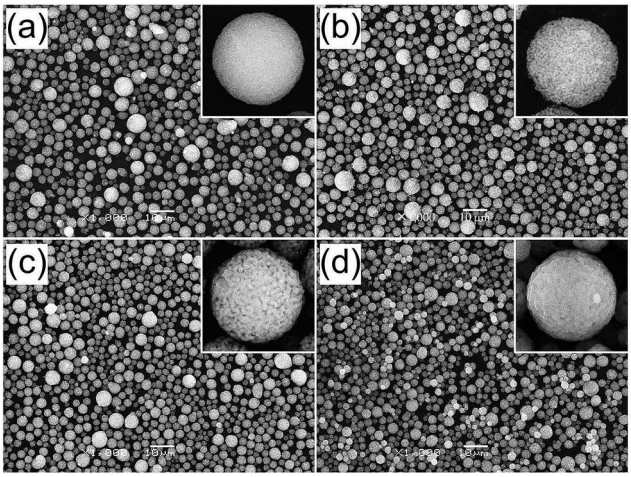

Fig. 3 SEM images of the (a) YAG:Ce^{3+} powders prepared by second-step spray drying process, and post-treated YAG:Ce^{3+} powders at the temperature of (b) 1200 °C, (c) 1300 °C, and (d) 1400 °C.

obtained by two-step spray drying were heat-treated at various temperatures between 1200 and 1400 °C. Fig. 3(b)–(d) show SEM images of the YAG:Ce^{3+} powders sintered at 1200, 1300, and 1400 °C, respectively. All the samples had an agglomeration-free spherical shape regardless of the heat-treatment temperature. As the heat-treatment temperature was increased, however, the particles gradually became smaller and denser, which was confirmed by measuring the particle size distributions (Fig. S3†). The average particle sizes were 3.3 ± 0.9, 2.7 ± 0.6, and 2.1 ± 0.4 μm for the samples with heat-treatment temperatures of 1200, 1300, and 1400 °C, respectively. To investigate the variations in porosity, specific surface areas of the particles were measured using nitrogen adsorption isotherms (Fig. S4†). The corresponding BET surface areas were 8.3, 3.6, and 2.3 $m^2\ g^{-1}$ for the particles that were calcined at 1200, 1300, and 1400 °C, respectively. The reduction in specific surface indicates that densification occurred with increasing sintering temperature.

Fig. 4 shows the excitation and emission spectra of the YAG:Ce^{3+} phosphor powders with post-spray-drying heat treatments between 1200 and 1400 °C. The excitation spectra displayed two bands with peaks at about 343 and 460 nm. All specimens showed typical band emission of YAG:Ce^{3+} in the range of 480–650 nm, with the maximum intensity at 535 nm under 460 nm blue-light excitation irrespective of the sintering temperature. These two excitation bands are attributed to the $4f^1 \rightarrow 5d^1$ transition of Ce^{3+}: as the excited 5d state of Ce^{3+} have many different energy components owing to the splitting of the crystal field, these two excitation bands observed at 343 nm and 460 nm are associated with the 4f → $5d(^2B_{1g})$ and 4f → $5d(^2A_{1g})$ transitions of Ce^{3+}, respectively. In excitation spectra, the peak intensity at 343 nm due to the 4f → $5d(^2B_{1g})$ transition was not enhanced when sintering temperatures were 1200 °C and 1300 °C. Usually, the shorter wavelength light shows the higher absorption coefficient. As

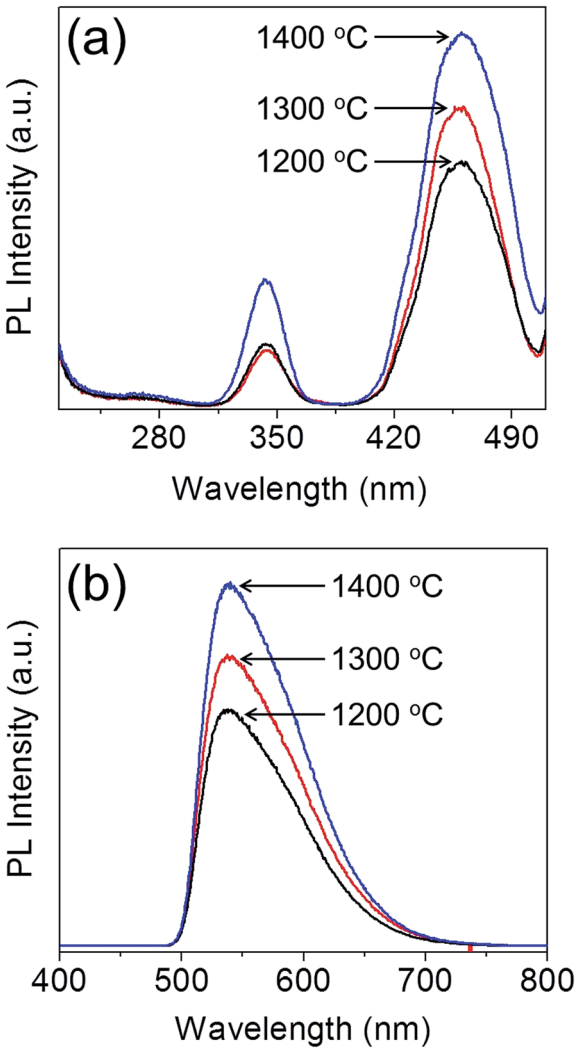

Fig. 4 Photoluminescence (a) excitation, and (b) emission spectra of the YAG:Ce^{3+} phosphor powders formed at the various sintering temperatures.

a result, high-energy photons could be absorbed within the surface regions of materials. As shown in Fig. 3, our samples are micron-sized particles, but porous. In addition, the primary particles have the size of dozens nanometers when post-treatment temperatures are lower than 1300 °C. That is, a lot of surface defects could exist, which seems to be the reason that the excitation band at 343 nm do not increase when the sintering temperatures were 1200 and 1300 °C. When the sintering temperature was 1400 °C, however, YAG:Ce powders are dense and primary particles are grown with large increase in the crystallite size. As a result, the surface defects are removed largely, and this leads to increase the excitation intensity at 343 nm at 1400 °C. The YAG:Ce^{3+} phosphor also showed one broad band emission, which was due to the overlap of two bands corresponding to the transitions from the lowest crystal-field component of $5d^1$ configuration to the spin–orbit split sublevels $^2F_{5/2}$ and $^2F_{7/2}$ of the $4f^1$ configuration of Ce^{3+} ions.[31] The emission intensity

of YAG:Ce^{3+} particles also increased with increasing sintering temperature. In general, the phase purity and crystallinity of YAG:Ce^{3+} phosphor strongly affect the emission properties. To check the crystal phase, XRD analysis was carried out, and the resulting XRD patterns are shown in Fig. S5.† The observed peaks are well matched to the $Y_3Al_5O_{12}$ phase (JCPDS card no. 88-2048), without any impurity phases such as $YAlO_3$ (YAP) and $Y_4Al_2O_9$ (YAM). According to a previous study in which YAG:Ce^{3+} was prepared by a solid-state method, the pure YAG phase can be formed at temperatures above 1400 °C.[32] For the YAG:Ce^{3+} powders that we prepared by two-step spray drying, the pure YAG phase was obtained at a lower temperature of 1200 °C. The XRD results indicate that all components of Y, Al, and Ce were homogeneously mixed in the YAG:Ce^{3+} precursor powder obtained after the first spray drying, which is in a good agreement with the elemental mapping results shown in Fig. 1(d) and 2(e). The crystallite sizes were 40, 48, and 78 nm for synthesized YAG:Ce^{3+} powders prepared with sintering temperatures of 1200, 1300, and 1400 °C, respectively. Moreover, the larger the crystallite size, the higher the crystallinity of the solid oxide. Therefore, the enhancement in the emission intensity of the YAG:Ce^{3+} powder was due to the increase in crystallinity with increasing sintering temperature. Based on the results achieved so far, the two-step spray-drying approach proposed in this work has been proved to be an effective way to produce spherical and dense YAG:Ce^{3+} particles with an average size of about 2 μm, which has the potential to be applied to the fabrication of white LEDs.

Conclusions

Dense and spherical YAG:Ce^{3+} particles with a narrow size distribution were prepared by a two-step spray-drying process. First, hollow YAG:Ce^{3+} precursor powder particles (organic–inorganic composites) were prepared by the first spray drying of an aqueous solution comprising nitrate precursors and citric acid. According to TG analysis, 550 °C was the optimal calcination temperature to completely eliminate the decomposable materials from the precursor powder. After simple ball milling, the calcined precursor powder could be easily turned into nanoparticles. According to the dot mapping of elements, it was clear that the Y, Al, O, and Ce components were distributed uniformly throughout the nanoparticles without any phase separation. The second drying using a suspension of the nanometer-sized precursor particles made it possible to obtain spherical, but porous, granular YAG:Ce^{3+} particles. After the post-spray-drying thermal treatment at a temperature between 1200 and 1400 °C to attain high crystallinity and activation of Ce^{3+} ions, densified and agglomeration-free spherical YAG:Ce^{3+} particles were obtained, and they had an average particle size of 2–3 μm depending on the temperature. These results demonstrate that the proposed two-step spray-drying process is a potential method for producing YAG:Ce^{3+} particles with spherical shape, narrow size distribution, and good luminescence properties. Finally, the YAG:Ce^{3+} powder displayed luminescence characteristics that are applicable for the fabrication of white LEDs based on blue-LED chips.

Acknowledgements

This work was supported by the National Research Foundation of Korea (NRF) grant funded by the Korea government (MEST) (no. 2012R1A2A2A02046367).

Notes and references

1 A. M. Khalid, G. Cossu, R. Corsini, P. Choudhury and E. Ciaramella, *IEEE Photonics J.*, 2012, **4**, 1465.
2 Y. Shi, G. Zhu, M. Mikami, Y. Shimomura and Y. Wang, *Opt. Mater. Express*, 2014, **4**, 280.
3 R. Zhang and X. Wang, *J. Alloys Compd.*, 2011, **509**, 1197.
4 S. Nishiura, S. Tanabe, K. Fujioka and Y. Fujimoto, *Opt. Mater.*, 2011, **33**, 688.
5 Y. Narukawa, M. Ichikawa, D. Sanga, M. Sano and T. Mukai, *J. Phys. D: Appl. Phys.*, 2010, **43**, 354002.
6 R. S. P. Scholtter, *Appl. Phys. A: Mater. Sci. Process.*, 1997, **64**, 417.
7 R. Mueller-Mach, G. O. Mueller, M. R. Krames and T. Trottier, *IEEE J. Sel. Top. Quantum Electron.*, 2002, **8**, 339.
8 P. Ghigna, S. Pin, C. Ronda, A. Speghini, F. Piccinelli and M. Bettinelli, *Opt. Mater.*, 2011, **34**, 19.
9 R. Zhang, H. Lin, Y. Yu, D. Chen, J. Xu and Y. Wang, *Laser Photonics Rev.*, 2014, **8**, 158.
10 C. Won, H. Nersisyan, H. Won, J. Lee and K. Lee, *J. Alloys Compd.*, 2011, **509**, 2621.
11 F. Yuan and H. Ryu, *Mater. Sci. Eng., B*, 2004, **107**, 14.
12 J. McKittrick, L. Shea, C. Bacalski and E. Bosze, *Displays*, 1999, **19**, 169.
13 R. Kasuya, T. Isobe, H. Kuma and J. Katano, *J. Phys. Chem. B*, 2005, **109**, 22126.
14 Y. Pan, M. Wu and Q. Su, *J. Phys. Chem. Solids*, 2004, **65**, 845.
15 X. Li, H. Liu, J. Wang, H. Cui and F. Han, *Mater. Res. Bull.*, 2004, **39**, 1923.
16 Y. C. Kang, I. W. Lenggoro, S. B. Park and K. Okuyama, *Mater. Res. Bull.*, 2000, **35**, 789.
17 M. S. Tsai, W. C. Fu, W. C. Wu, C. H. Chen and C. H. Yang, *J. Alloys Compd.*, 2008, **455**, 461.
18 H. K. Yang and J. H. Jeong, *J. Phys. Chem. C*, 2009, **114**, 226.
19 I. Matsubara, M. Paranthaman, S. Allison, M. Cates, D. Beshears and D. Holcomb, *Mater. Res. Bull.*, 2000, **35**, 217.
20 G. Xia, S. Zhou, J. Zhang and J. Xu, *J. Cryst. Growth*, 2005, **279**, 357.
21 B. Hoghooghi, L. Healey, S. Powell, J. McKittrick, E. Sluzky and K. Hesse, *Mater. Chem. Phys.*, 1994, **38**, 175.
22 D. S. Jung, T. H. Hwang, S. B. Park and J. W. Choi, *Nano Lett.*, 2013, **13**, 2092.
23 R. López, F. González, M. P. Cruz and M. E. Villafuerte-Castrejon, *Mater. Res. Bull.*, 2011, **46**, 70.
24 A. B. D. Nandiyanto and K. Okuyama, *Adv. Powder Technol.*, 2011, **22**, 1.
25 X. Xiong, Z. Wang, H. Guo, X. Li, F. Wu and P. Yue, *Electrochim. Acta*, 2012, **71**, 206.

26 M. Vicent, E. Sánchez, I. Santacruz and R. Moreno, *J. Eur. Ceram. Soc.*, 2011, **31**, 1413.
27 J. S. Cho and Y. C. Kang, *RSC Adv.*, 2014, **4**, 25234.
28 J. S. Cho, S. M. Lee, K. Y. Jung and Y. C. Kang, *RSC Adv.*, 2014, **4**, 43606.
29 T. Han, S. Cao, D. Zhu, C. Zhao, M. Ma, M. Tu and J. Zhang, *Optik*, 2013, **124**, 3539.
30 W. Chen, D. Jo, Y. Song, T. Masaki and D. Yoon, *J. Lumin.*, 2014, **147**, 304.
31 A. Katelnikovas, J. Plewa, D. Dutczak, S. Möller, D. Enseling, H. Winkler, A. Kareiva and T. Jüstel, *Opt. Mater.*, 2012, **34**, 1195.
32 H. Shi, J. Chen, J. Huang, Q. Hu, Z. Deng, Y. Cao and X. Yuan, *Phys. Status Solidi A*, 2014, **211**, 1596.